Nano Energy (2015) 13, 58–66

Available online at www.sciencedirect.com

ScienceDirect

journal homepage: www.elsevier.com/locate/nanoenergy

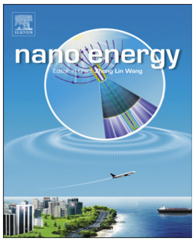

RAPID COMMUNICATION

Template-free synthesis of ultra-large V_2O_5 nanosheets with exceptional small thickness for high-performance lithium-ion batteries

Shuquan Liang[a], Yang Hu[a], Zhiwei Nie[a], Han Huang[c], Tao Chen[a], Anqiang Pan[a,b,*], Guozhong Cao[d,**]

[a]*School of Materials Science & Engineering, Central South University, Hunan 410083, PR China*
[b]*State Key Laboratory of Powder Metallurgy, Central South University, Hunan 410083, PR China*
[c]*Institute of Super Microstructure and Ultrafast Process in Advanced Materials, School of Physics and Electronics, Central South University, Hunan 410083, PR China*
[d]*Department of Materials Science & Engineering, University of Washington, Seattle, WA 98185, USA*

Received 31 August 2014; received in revised form 15 January 2015; accepted 30 January 2015

KEYWORDS
Ultra-large nanosheets;
Free-standing;
VO_2(B);
V_2O_5;
Lithium-ion batteries

Abstract

Similar to graphene, transition metal oxide nanosheets have attracted a lot of attention recently owning to their unique structural advantages, and demonstrated promising chemical and physical properties for various applications. However, the synthesis of transition metal oxide nanosheets with controlled size and thickness remains a great challenge for both fundamental study and applications. The present work demonstrates a facile solvothermal synthesis of ultra-large (over 100 μm) VO_2(B) nanosheets with an exceptionally small thickness of only 2–5 nm corresponding to 3–8 layers of (001) planes. It can be readily transferred into V_2O_5 with well retained nanosheet structures when calcined, which exhibit remarkable rate capability and great cycling stability. Specifically, the as-synthesized vanadium pentoxide nanosheets deliver a specific discharge capacity of 141 mA h g^{-1} at a current density of 0.1 A g^{-1}, which is 96% of its theoretical capacity (147 mA h g^{-1}) for one Li^+ ion intercalation/removal per formular within a voltage window of 2.5–4 V. Even at an extreme-high current density of 5 A g^{-1}, it still can exhibit a high specific discharge capacity of 106 mA h g^{-1}. It is worthy to note that the V_2O_5 nanosheets electrode can retain 92.6% of the starting specific discharge capacity after 500 discharge/charge cycles at the current density of 1.5 A g^{-1}.

---

*Corresponding author at: School of Materials Science & Engineering, Central South University, Hunan, 410083, PR China.
**Corresponding author.
E-mail addresses: pananqiang@csu.edu.cn (A. Pan), gzcao@u.washington.edu (G. Cao).

http://dx.doi.org/10.1016/j.nanoen.2015.01.049
2211-2855/

Introductions

Recently, two-dimensional (2D) materials have drawn considerable attention because of their distinctive electronic, photonic, magnetic and mechanical properties and promising applications in sensors, [1] catalysts, [2] and energy storage and conversion devices [3-7]. Intrigued by such advantages, great effort has been devoted to fabricate thinner and larger 2D nanosheets through facile methods. To date, delamination or exfoliation is the most commonly developed approaches to prepare lamellar inorganic materials. However, it usually requires the modification of interlamellar environment and the appropriate selection of the solvent system, whereas it always takes over one week to get highly exfoliated nanosheets due to the tedious long-term aging and sonification process [8-10]. Moreover, the lateral scale of two-dimensional nanosheets prepared by chemical exfoliation is highly dependent on the pristine bulk materials used and the employed violent sonification would break the nanosheets into smaller pieces than the raw bulk materials itself. Therefore, it is still a big challenge to obtain ultra-large nanosheets with ultra-thin thickness.

Among the transition metal oxides, V_2O_5 has attracted considerable attention as potential cathode materials in lithium ion batteries (LIBs) in the last decades because of their high theoretical capacity [11-13], good reversibility, easy preparation and abundant resources in store [14-16]. For example, a theoretical capacity of 294 mA h g^{-1} can be obtained when two Li^+ ions take part in the intercalation process. With a layered structure [17,18], V_2O_5 readily accommodate Li^+ ions insertion and removal, thus shows a good reversibility within the voltage range of 2-4 V. However, its electrochemical performances are suffered from the low Li^+ diffusion efficiency and poor electron conductivity [19]. Nanostructured materials are believed to be an effective way to solve the problems because of the nanoscale effect, which includes the enlarged surface area, reduced Li^+ diffusion distance and shortened electron transportation distance. So far, various nanostructured materials have been fabricated to demonstrate the enhanced electrochemical performances, such as nanoarrays, [19] nanorods, [20] nanowires, [21] nanobelts, [22,23] nanosheets [8,24,25] and three-dimensional hollow micro/nanospheres [26]. Moreover, the surface energy and surface defects of the active material is believed to contribute to the superior electrochemical performances [27,28]. Lou et al. [28] reported the TiO_2 microspheres with (001) exposed faces exhibit fast reversible lithium storage. In order to acquire desired electrochemical properties, such as high rate capability and good cyclic stability, preferial grown materials with good structural integrity and facile Li^+ ions diffusion paths during the charge/discharge process would be a good choice. Nanosheet-structured materials with exceptional small thickness and ultralarge lateral size may be of great interest to the fundamental research or practical applications, because the exceptional small thickness of the nanosheet can ensure the high rate capability and the ultralarge lateral size can keep the structural integrity upon cycling. Although Pan et al. [29] have reported many nanosheet-assembled 3D hollow microspheres, the synthesis of freestanding 2D V_2O_5 are rarely reported. Recently, V_2O_5 nanosheets with several micrometers were fabricated by a top-down exfoliation method, which demonstrated good electrochemical performance [8]. However, the tedious exfoliation process by sonification technique requires long-term treatment and the obtained nanosheets are easily broken into small pieces. Thus, to develop new effective strategies to synthesis ultralarge nanosheets with ultrathin thickness is of great interest to the fundamental research and practical applications.

Herein, a bottom-up solvothermal approach has been developed for the synthesis of ultra-large VO_2(B) nanosheets with a lateral size over 100 μm. To the best of our knowledge, the nanosheets are the largest among the nanosheets ever reported. Moreover, the nanosheets are layer-by-layer stacked with an ultrathin thickness of 2-5 nm. After calcination in air, the V_2O_5 nanosheets with well retained structures can be obtained. As cathode materials for lithium ion batteries, the as-prepared V_2O_5 nanosheets electrodes exhibit excellent rate capability and remarkable cyclic stability.

Experimental section

Preparation of VO_2(B) uniform ultrathin nanosheets

All of the chemical reagents were of analytical grade and used without further purification. In a typical synthesis, 50 mg vanadium pentoxide (V_2O_5, ≥99.0%, Tianjin Damao Reagent Co., Ltd.) was dispersed in 5 ml deionized water by 5 min ultrasonic treatment. Then, 10 mL hydrogen peroxide (H_2O_2, ≥30%, Sinopharm Chemical Reagent Co., Ltd.) was added into the above suspension under vigorous stirring at room temperature, as it gradually turned into a bright yellow solution. And 5 min later, 10 mL isopropanol ($(CH_3)_2CHOH$, ≥99.7%, Sinopharm Chemical Reagent Co., Ltd.) was added and vigorously stirred for another 5 min before it was transferred into a 50 mL Teflon container, which was sealed in a steel autoclave and kept in an electrical oven at 180 °C for 6 h. After cooling down naturally, the blue precipitate was washed with pure ethanol by centrifiguing for three times to remove the organic solvent, and then the blue product was collected by filtering and dried in room temperature naturally to get the VO_2 nanosheets which can be peeled off as a whole piece (Figure S1).

Preparation of V_2O_5 ultrathin nanosheets

The uniform V_2O_5 nanosheets were obtained by calcining the solvothermally prepared VO_2(B) nanosheets in air at 350 °C for 2 h with a heating ramp of 1 °C min^{-1}.

Materials characterization

Crystallographic phases of both products were investigated by powder X-ray diffraction (XRD, Rigaku D/max2500) using CuKα radiation(λ=1.54178 Å). The samples were scanned in the range between 10 °and 80°(2θ) with a step size of 0.02°. Morphologies of the samples were examined by field-emission scanning electron microscope (FESEM, SIRION 200) and transmission electron microscope (TEM, JEOL JEM-2100 F). Tapping mode atomic force microscope (AFM) images were obtained on

Agilent Technologies 5500 under ambient conditions. For SEM and AFM characterization, both samples (VO_2(B) and V_2O_5) were dispersed in ethanol by ultrasonic treatment before they were dripped on the smooth surface of silicon wafer. Fourier-transform infrared spectra (FTIR) were recorded from 4000 to 400 cm^{-1} on a Nicolet 6700 spectrometer (Thermo Electron Scientific Instruments, USA), the sample was milled with KBr before it was compressed into a pellet for charaterization. Raman spectroscopy was performed using a LabRAM HR800 spectrometer (Horiba Jobin Yvon S.A.S), under the blue laser excitation with 488 nm wavelength and 10 mW power. TG and DSC test was carried out on a STA449C (NETZSCH, Germany) from room temperature to 600 °C with a heating ramp of 5 °C min^{-1}.

Electrochemical measurements

The working electrode slurry was prepared by dispersing V_2O_5 active material, acetylene black and poly (vinylidene fluoride) (PVDF) binder in N-methyl pyrrolidone with a weight ratio of 70:20:10. The slurry was spread on aluminum foil, which served as current collector in the cathode, and then was dried in a vacuum oven at 100 °C overnight prior to cells assembly. All cells was assembled in a glove-box filled with pure argon, using lithium foil as the counter and reference electrode, and 1.0 M $LiPF_6$ in ethyl carbonate/diethyl carbonate/dimethyl carbonate (EC/DEC/DMC, 1:1:1v/v/v ratio) as the electrolyte. The galvanostatic charge/discharge performances of the electrodes were evaluated at room temperature using a Land Battery Tester (Land CT 2001 A, China) within the voltage range of 2.5–4 V (vs. Li/Li^+). And the calculation of specific capacity of the V_2O_5 cathode is based on the mass of active materials (V_2O_5) only. Cyclic voltammetry (CV) was tested with an electrochemical workstation (CHI660C, China) at a scan rate of 0.05 mV s^{-1} in the voltage range of 2.5–4 V (vs. Li/Li^+). The electrochemical impedance spectrometry (EIS) was are carried out on a ZAHNER-IM6ex electrochemical workstation (ZAHNER Co.,Germany) in the frequency range of 100 kHz to 10 mHz.

Results and discussions

The detailed color changes of the samples for each step are clearly presented in Figure S1. The color change from orange to a bright yellow solution was attributed to the reaction between V_2O_5 powders and H_2O_2 to form V_2O_5 sol. Adding isopropanol in the open beaker would not cause aparent color change at room temperature. After solverothermally treated at 180 °C for 6 h, dark blue precipitates were obtained (Figure S1d), the color of which is quite similar to that of VO_2. The blue precipitates can be easily re-dispersed in alcohol by ultrasonic treatment. The homogeneous blue suspension was filtered and peeled off to get a disk (see Figure S1g). After annealing the blue disk in air at 350 °C for 2 h, the color changed into yellow color, which is the typical color of V_2O_5.

The as-obtained blue disk (Figure S1g) was characterized by the powder X-ray diffraction (XRD) technique (Figure 1a) and the result is quite similar to that of the single layered VO_2 (B) nanosheets reported by Xie et al. previously [9]. The observed dark blue color also corresponds well with the color of VO_2(B). It is believed the V_2O_5 powder can react with H_2O_2 to form V_2O_5 sol first [30], which is then reduced by isopropanol in the solvothermal process [29]. The reduction of V_2O_5 sol by achohol has also been reported previously [31]. Compared with the standard pattern of monoclinic VO_2(B) (JCPDS Card no.81–2392: $C2/m$ (12), a=12.093 Å, b=3.702 Å, c=6.433 Å), the product only exhibits strong (001), (002) and (003) peaks. So it is highly possible that the products are composed of pure ultrathin layered VO_2(B) with a well-defined (00l) crystal plane orientation. To confirm this, more structural information of the as-synthesized product was investigated by FTIR (Figure S2) and Raman spectroscopy (Figure S3), and both results were highly consistent with previously reported VO_2(B) nanorods [32], which strongly corroborated the conclusion that the as-synthesized solvothermal product was VO_2(B) nanosheets. And the field-emission scanning electron microscope (FESEM) images (Figure 1b and c) confirm that the obtained precursor is composed of ultra-large nanosheets with a lateral dimension over 100 μm. The existence of isopropanol is essential to obtain the nanosheet structures. When the isopropanol was replaced by distilled water, keeping other parameters unchanged, only an orange solution was formed without any precipitates. With the addition of isopropanol, the V_2O_5 sols is reduced to VO_2(B) species, which will self-assemble into VO_2(B) nanosheets in order to reduce their surface energy. The lateral scale of the obtained nanosheets is much larger than other VO_2(B) nanosheets reported previously [9,31]. The layer stacking structures are clearly revealed in the transmission electron microscope (TEM) images (Figure 1c and d), which indicates the nanosheets are stacked with each other. The higher magnification TEM image (see Figure S4), as indicated by the numbers, gives a much clear edges information about the layer-by-layer stacked nanosheet structures. High-resolution TEM characterization (Figure 1e) clearly reveals the nanosheet is a single-crystalline, and the lattice fringe of 0.353 nm corresponds well with the neighboring distance between the (110) planes of monoclinic VO_2(B). And the selected area electron diffraction (SAED) pattern of the VO_2(B) nanosheets confirms the high crystallinity of the nanosheets and the nanosheets are grown preferentially along (00l) planes. The formation of this (00l) orientation can be attributed to the higher energy and more atoms possessed by the most closely packed (00l) crystal planes and the large number of O–H bond and V–O bond groups on its surface [33]. With all these structural information, it is quite reasonable to conclude that the as-synthesized products are pure monoclinic VO_2(B) nanosheets with a highly (00l) orientation. According to the above characterization results, the formation mechanism of VO_2(B) nanosheets is proposed as follows: the V_2O_5 sols prepared from H_2O_2 and V_2O_5, were reduced to VO_2 nanoparticles by alcohol at the interface between V_2O_5 sol and isopropanol during the solvothermal process. The in situ formed VO_2 nanoparticles self-assembled into ultralarge nanosheets with the preferential growth along (00l) in order to get a more stable state.

After annealing in air at 350 °C for 2 h, the VO_2(B) ultrathin nanosheets can be safely transferred into V_2O_5 nanosheets with good morphology reservation. The TG and DSC results (see Figure S5) indicate a sharp weight increase of VO_2 nanosheets at around 400 °C due to the oxidation of VO_2 into V_2O_5. The existence of higher temperature for the oxidation than 350 °C used in this work can be attributed to the fast ramping rate and

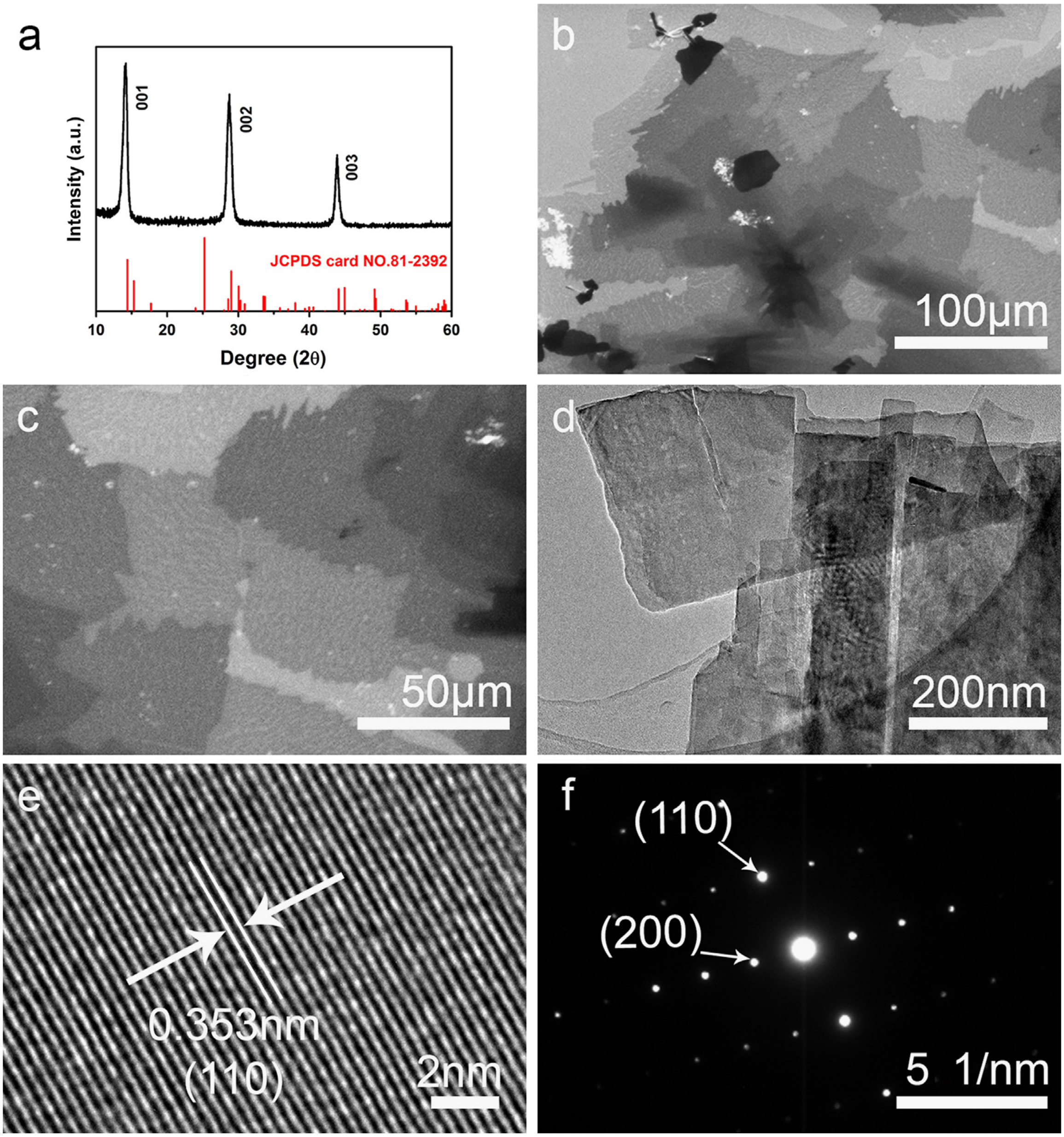

Figure 1 XRD pattern (a), SEM images (b, c), TEM image (d), HRTEM image (e) and SAED image (f) of VO_2(B) nanosheets prepared by solvothermal method.

short dwell time. Figure 2a shows the XRD pattern of the calcination product, which can be indexed to pure orthorhombic V_2O_5 phase (JCPDS Card no.41-1426: *Pmnm* (59), a=11.516 Å, b=3.5656 Å, c=4.3727 Å). Although some small peaks were detected, the peak around 20° correspond to (001) plane outstanded from others with a much stronger intensity, and (002) plane made the third strongest peak, slightly weaker than the (101) plane. This result indicates that the strong orientation is well-retained from the VO_2(B) precursor upon calcinations. As shown in the FESEM image (Figure 2b), the lamellar structure can be retained from VO_2(B) nanosheets when a slow temperature ramping rate of 1 °C $\min^{-1}$ is applied. The resulting V_2O_5 nanosheets are still ultrathin, and some of which can retain the large lateral dimension. The finding of the curling up at the edges of the nanosheets suggests their ultrathin feature and good flexibility. The TEM image (see Figure 2c) clearly reveals that the nanosheet morphology of the V_2O_5, except its edge becomes a little jagged in the process of calcinations compared with the precursor.The high-resolution TEM (Figure 2d) suggests that the V_2O_5 nanosheet is of single-crystalline and the lattice fringe of 0.576 nm can be assigned to the (200) plane.

To further study the thickness of the solvothermal VO_2(B) nanosheets and its calcination product, atomic force microscope (AFM) were employed to characterize the stacking feature of the nanosheets. As shown in Figure 3a, the large VO_2(B) nanosheet is well presented and the thickness is detected to be 5.2 nm. Figure 3b clearly displays the parallel stacking structures, the thickness of which is in the range of 2–5 nm (Figure 3c). According to the

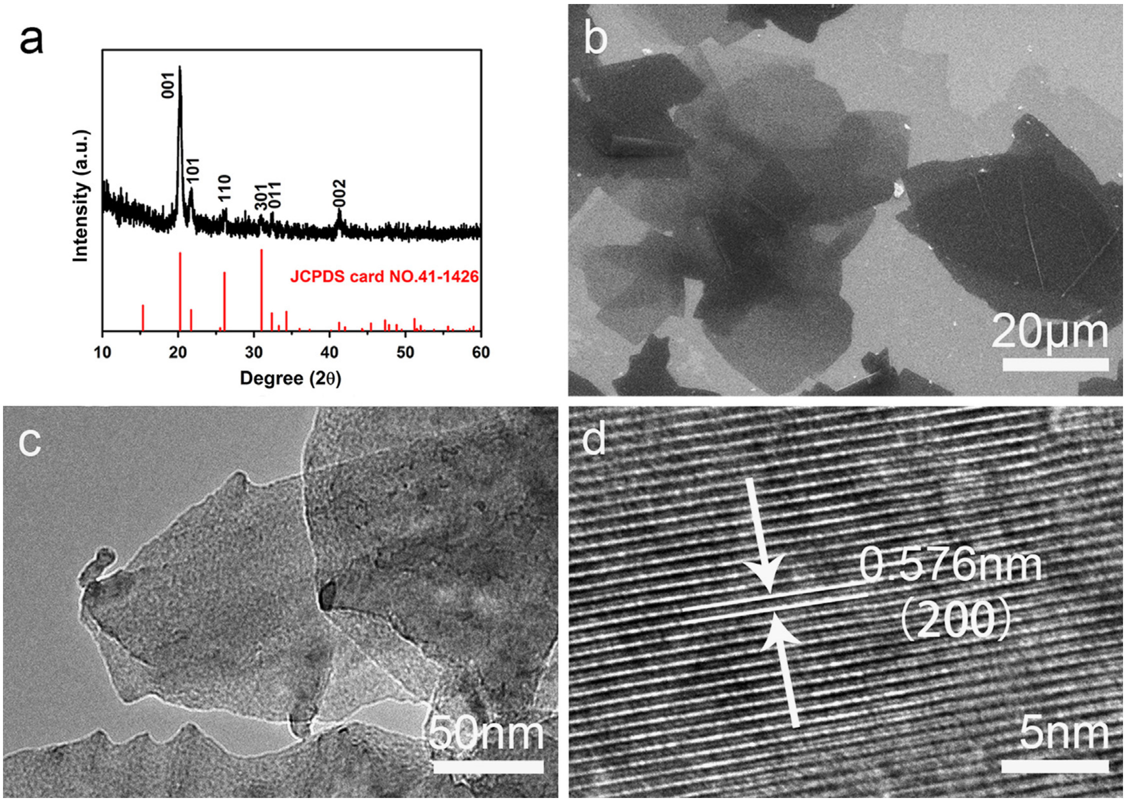

Figure 2 XRD pattern (a), SEM image (b), TEM image (c) and HRTEM image (d) of the V_2O_5 nanosheets synthesized by calcinations of the precursor VO_2(B) nanosheets.

XRD and TEM results, the nanosheets are of single crystalline and preferential grow along (001) plane, thus the ultra-large nanosheets are of the thickness of 3-8 layers (calculation was based on the thickness of nanosheets provided by the AFM results and the interplanar spacing data of (001) plane from the JCPDS Card no.81-2392). The annealed products are also investigated by AFM and the result is shown in Figure 3d, e and f. Both large nanosheets and parallel stacked structures are distinctly revealed, which has a similar feature to the VO_2(B) nanosheets. The thickness of the large nanosheet is around 4 nm and the thickness of the parallel stacked nanosheets is about 3-5 nm. The result demonstrate that not only the overall nanosheet morphology is well reserved, but also the space between the neighboring nanosheets is retained. The ultra large nanosheets and the layer-by-layer stacking structures are expected of advantages to obtain good electrochemical performance for lithium ion batteries.

The V_2O_5 nanosheets were assembled into coin cells to evaluate their structural advantages in lithium ion batteries. The V_2O_5 nanosheets electrode was first studied by cyclic voltammetry (CV) test within the voltage range of 2.5-4 V vs. Li/Li$^+$. As Figure 4a shows, the first five consecutive CV curves are almost identical and no obvious decay is observed, which suggests the remarkable reversibility of the electrode upon cycling. The observation of the two cathodic peaks at the potentials of 3.38 V and 3.17 V indicate the multi-step lithium-ion insertion process in the active materials, and correspond to the phase changes from α-V_2O_5 to ε-$Li_{0.5}V_2O_5$, and ε-$Li_{0.5}V_2O_5$ to δ-LiV_2O_5, respectively [15,16]. While the anodic peaks at the potentials of 3.25 V and 3.43 V correspond to the de-intercalation of lithium and the successive backward transformation of the phase from δ-LiV_2O_5 to ε-$Li_{0.5}V_2O_5$, and from ε-$Li_{0.5}V_2O_5$ to α-V_2O_5, respectively [34]. The narrow potential gaps between the cathodic and anodic peaks demonstrate the low polarization between the electrode and electrolyte.

The galvanostatic charging/discharging measurement was carried out to investigate the long-term cyclic stability of the V_2O_5 nanosheet electrodes. A maximum capacity of 141 mA h g^{-1} can be delivered at the current density of 100 mA g^{-1} (see Figure S6a), which is very close to the theoretical capacity of 147 mA h g^{-1} for one Li$^+$ ion intercalation per formula. Multiple voltage plateaus related to the lithium ion intercalation and de-intercalation are clearly observed. The two plateaus, at approximately 3.35 V and 3.15 V, are attributed to the phase transitions from α-V_2O_5 to ε-$Li_{0.5}V_2O_5$, and to δ-LiV_2O_5, respectively. The large overlap of the discharge and charge curves indicate the good cyclic stability of the V_2O_5 nanosheet electrodes (see Figure S6b). Figure 4b shows the cycling behavior of the V_2O_5 electrodes at the current densities of 300, 1500 and 3000 mA g^{-1} in the voltage range of 2.5-4.0 V vs. Li/Li$^+$. The maximum specific discharge capacities at the 2nd cycles are 135 mA h g^{-1}, 125 mA h g^{-1} and 116 mA h g^{-1}, respectively, with a corresponding capacity retention of 93.8%, 92.6%, and 87.1% after 200 cycles. The coulombic efficiency is close to 100% in the whole discharge/charge process. To further study the long-term capacity retention capability, the V_2O_5 nanosheet electrode was cycled at 1500 mA g^{-1} for 500 cycles. It is astounding that 92.6% of the initial capacity can be retained with an average

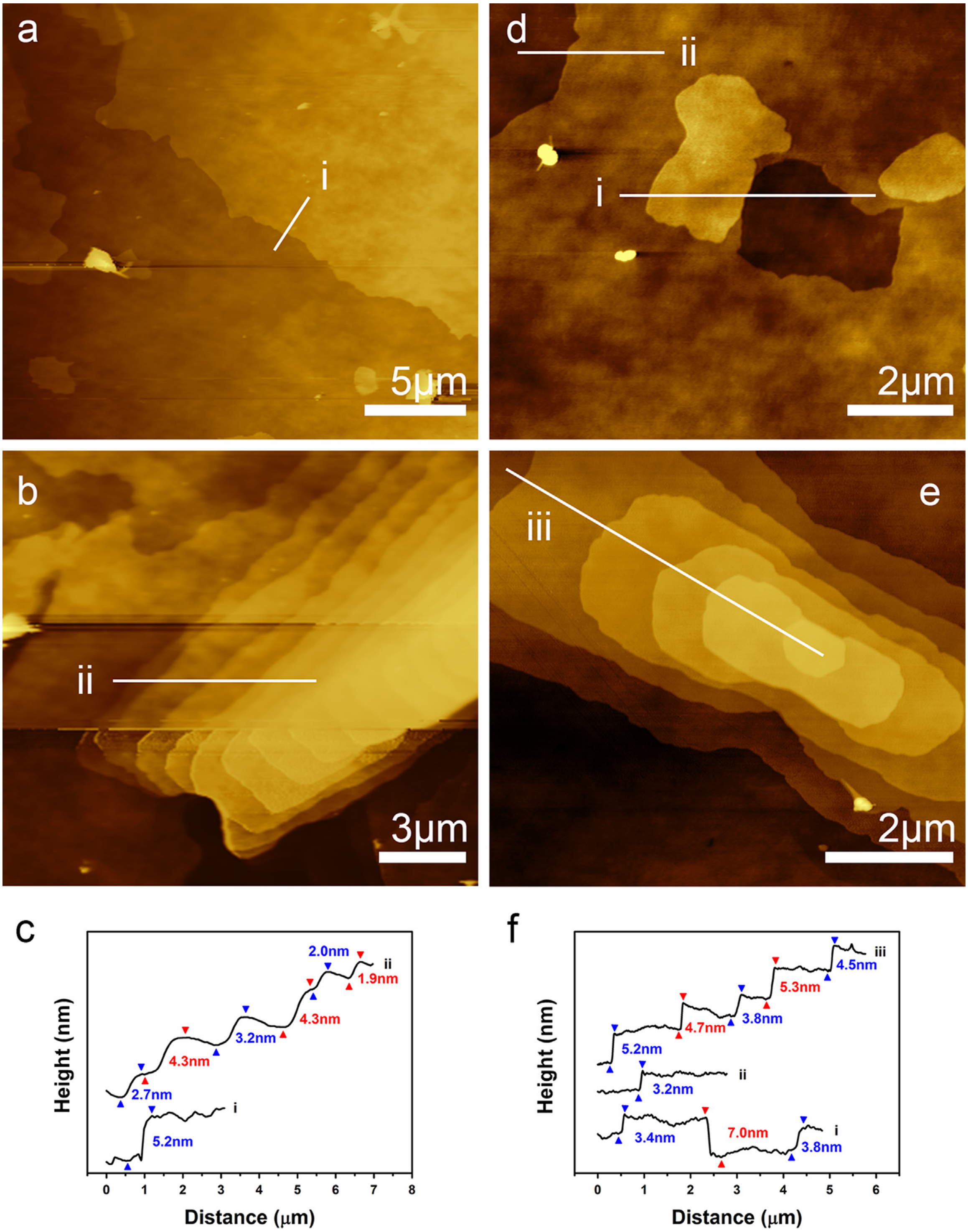

Figure 3 Characterizations of the ultra-thin feature of the products: (a) an individual sheet and (b) multi-layer stacking structures of the VO_2(B) nanosheets and its corresponding (c) height profiles; (d) single nanosheet and (e) multi-layer stacking structures of the V_2O_5 nanosheets and its corresponding (f) height profiles.

capacity fading rate of 0.015% per cycle (see Figure S7). The cycling performance is better than the nanosheet-assembled hollow V_2O_5 microspheres [29]. The excellent cyclic stability can be attributed to the extremely large lateral size and the layer-by-layer stacking structures, which can better keep the structural integrity upon cycling.

Figure 4c and d show the rate capability and their corresponding discharge/charge curves of the V_2O_5 nanosheet electrode at various current densities, respectively. An initial discharge capacity of 139 mA h g^{-1} can be delivered at 0.1 A g^{-1}, which decreases to 138, 136, 133, 129, 119 and 103 mA h g^{-1}, at 0.2, 0.4, 0.8, 1.6, 3.2 and

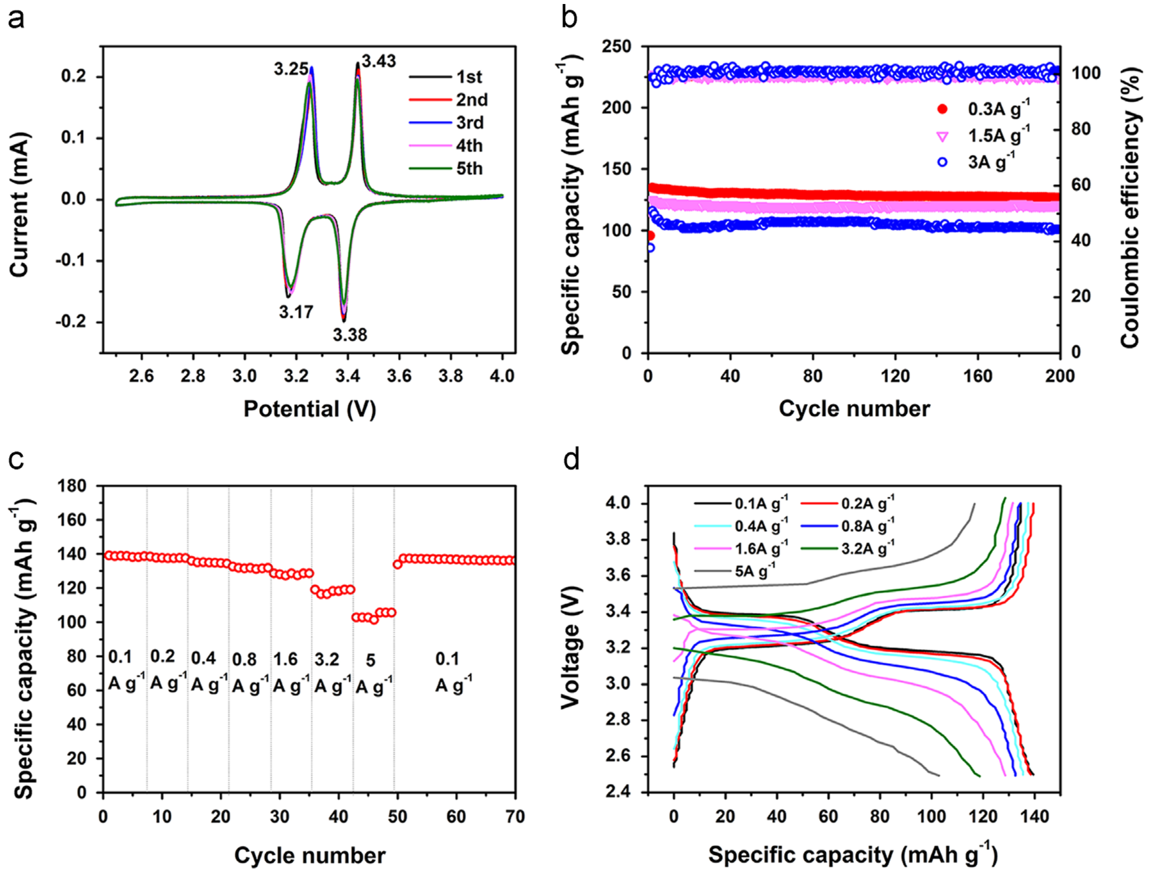

Figure 4 The electrochemical performance of the V_2O_5 nanosheets: (a) the first 5 consecutive cyclic voltammograms; (b) the first 200 cycles of galvanostatic discharge-charge test conducted at various current densities; (c) the specific capacity as a function of cycle number in the rate charge and discharge cycling test and (d) the corresponding voltage-specific capacity profiles of the first cycles in various current densities.

$5\ A\ g^{-1}$, respectively. When the current was re-set to $0.1\ A\ g^{-1}$, a specific capacity of $137\ mA\ h\ g^{-1}$ can be restored. It is worth mention that the V_2O_5 nanosheets can still deliver a high and stable specific capacity of $103\ mA\ h\ g^{-1}$ at an extremely high current density of $5\ A\ g^{-1}$. Figure 4d shows the corresponding discharge/charge curves at various current densities. The plateaus on the discharge/charge curves are clearly presented when the current densities are smaller than $3.2\ A\ g^{-1}$. The plateaus are almost identical at relatively low current densities ($0.1\ A\ g^{-1}$, $0.2\ A\ g^{-1}$, $0.4\ A\ g^{-1}$). Although the plateaus become obscure, the electrode can still deliver high specific capacities as the current density increased to $3.2\ A\ g^{-1}$ and $5\ A\ g^{-1}$. The rate performance is comparative to the recently reported V_2O_5 nanosheets [8], and much higher than the previous reported nanosheets [24,25]. According to the electrochemical impedance spectroscopy (EIS) measurement results (see the detailed analysis in Figure S8), a small charge transfer resistance of $82.14\ \Omega$ is detected, which indicates the ultra-thin nanosheets can facilitate the lithium ions insertion and removal process upon cycling. Compared with other morphologies of nanostructured V_2O_5 cathodes, the electrochemical performance is much better than the previous reported results for nanorods [20,35], nanowires [21,36], and 3D self-assembled microspheres [37]. The excellent rate performance and remarkable cyclic stability can be contributed to the structural advantageous of its uniform 2D ultrathin nanosheet with ultra-large lateral size: (1) the void space between the nanosheets can facilitate the penetration of electrolyte; (2) the ultra-thin feature can reduce the Li^+ ions diffusion distance and electron transportation distance; (3) the flexibility of nanosheets can accommodate the volume changes caused by the repeated lithium ions insertion and removal; (4) the ultra-large nanosheets and the layer-by-layer stacking structures can better keep the integrity of the nanosheet electrodes.

Conclusions

In summary, a facile one-pot solvothermal method has been developed to synthesize uniform VO_2(B) ultrathin nanosheets with a lateral size over $100\ \mu m$, which can be readily transformed into V_2O_5 nanosheets with good structural revervation, including the exceptionally small thickness and the large lateral size by calcination in air. Moreover, the layer-by-layer stacking structures are well revealed. As cathode materials for lithium ion batteries, the resulting V_2O_5 nanosheets exhibite remarkable electrochemical performances, including high reversible capacity, good cyclic stability and great rate capability. The V_2O_5 nanosheet can still deliver a high reversible capacity of $106\ mA\ h\ g^{-1}$ even at a super-high current density of $5\ A\ g^{-1}$ and it can retain 92.6% of its starting capacity at the current density of 1.5 A g^{-1} after 500 cycles. The exceptional electrochemical performance can be attributed to the layer-by-layer stacked ultra-large nanosheets with exceptionally small thickness, which can keep the structural integrity and kinetically favorable for redox reactions upon cycling. The results deomonstrate that the V_2O_5 nanosheets electrodes are promising alternative cathode materials for high-performance LIBs.

Acknowledgments

This work was supported by the National High Technology Research and Development Program of China (863 Program) (No. 2013AA110106), the National Natural Science Foundation of China (No. 51374255, 51302323), Program for New Century Excellent Talents in University (NCET-13-0594), Research Fund for the Doctoral Program of Higher Education of China (No. 201301621200), Natural Science Foundation of Hunan Province, China (14JJ3018), Lie-Ying and Sheng-Hua Program of Central South University, and State Key Laboratory of Powder Metallurgy, Central South University. The AFM measurement was conducted at Institute of Super Microstructure and Ultrafast Process in Advanced Materials, School of Physics and Electronics, Central South University.

Appendix A. Supporting information

Supplementary data associated with this article can be found in the online version at http://dx.doi.org/10.1016/j.nanoen.2015.01.049.

References

[1] S. Wu, Z. Zeng, Q. He, Z. Wang, S.J. Wang, Y. Du, Z. Yin, X. Sun, W. Chen, H. Zhang, Small 8 (2012) 2264-2270.
[2] M. Choi, K. Na, J. Kim, Y. Sakamoto, O. Terasaki, R. Ryoo, Nature 461 (2009) 246-249 (U120).
[3] C. Xu, Y. Zeng, X. Rui, N. Xiao, J. Zhu, W. Zhang, J. Chen, W. Liu, H. Tan, H.H. Hng, Q. Yan, ACS Nano 6 (2012) 4713-4721.
[4] J. Liu, J. Jiang, C. Cheng, H. Li, J. Zhang, H. Gong, H.J. Fan, Adv. Mater. 23 (2011) 2076-2081.
[5] T.-J. Kim, C. Kirn, D. Son, M. Choi, B. Park, J. Power Sources 167 (2007) 529-535.
[6] J.S. Chen, X.W. Lou, Electrochem. Commun. 11 (2009) 2332-2335.
[7] D. Yang, Z. Lu, X. Rui, X. Huang, H. Li, J. Zhu, W. Zhang, Y.M. Lam, H.H. Hng, H. Zhang, Q. Yan, Angew. Chem. Int. Ed. 53 (2014) 9352-9355.
[8] X. Rui, Z. Lu, H. Yu, D. Yang, H.H. Hng, T.M. Lim, Q. Yan, Nanoscale 5 (2013) 556-560.
[9] L. Liu, T. Yao, X. Tan, Q. Liu, Z. Wang, D. Shen, Z. Sun, S. Wei, Y. Xie, Small 8 (2012) 3752-3756.
[10] T. Yao, L. Liu, C. Xiao, X. Zhang, Q. Liu, S. Wei, Y. Xie, Angew. Chem. Int. Ed. 52 (2013) 7554-7558.
[11] Y. Wang, G.Z. Cao, Adv. Mater. 20 (2008) 2251-2269.
[12] D.W. Liu, G.Z. Cao, Energy Environ. Sci. 3 (2010) 1218.
[13] Q.F. Zhang, E. Uchaker, S.L. Candelaria, G.Z. Cao, Chem. Soc. Rev. 42 (2013) 3127-3171.
[14] X.-F. Zhang, K.-X. Wang, X. Wei, J.-S. Chen, Chem. Mater. 23 (2011) 5290-5292.
[15] R.J. Cava, A. Santoro, D.W. Murphy, S.M. Zahurak, R. M. Fleming, P. Marsh, R.S. Roth, J. Solid State Chem. 65 (1986) 63-71.
[16] Y.S. Hu, X. Liu, J.O. Muller, R. Schlogl, J. Maier, D.S. Su, Angew. Chem. Int. Ed. 48 (2009) 210-214.
[17] L. Abello, E. Husson, Y. Repelin, G. Lucazeau, Spectrochim. Acta Part A Mol.. Spectrosc. 39 (1983) 641-651.
[18] D.W. Murphy, P.A. Christian, F.J. DiSalvo, J.V. Waszczak, Inorg.. Chem. 18 (1979) 2800-2803.
[19] D. Chao, X. Xia, J. Liu, Z. Fan, C.F. Ng, J. Lin, H. Zhang, Z.X. Shen, H.J. Fan, Adv. Mater. 26 (2014) 5733 (5733).
[20] A.Q. Pan, J.-G. Zhang, Z. Nie, G. Cao, B.W. Arey, G. Li, S.-q. Liang, J. Liu, J. Mater. Chem. 20 (2010) 9193-9199.
[21] J.W. Lee, S.Y. Lim, H.M. Jeong, T.H. Hwang, J.K. Kang, J.W. Choi, Energy Environ. Sci. 5 (2012) 9889-9894.
[22] Y. Wang, H.J. Zhang, W.X. Lim, J.Y. Lin, C.C. Wong, J. Mater. Chem. 21 (2011) 2362-2368.
[23] M.L. Qin, Q. Liang, A.Q. Pan, S.Q. Liang, Q. Zhang, Y. Tang, X. P. Tan, J. Power Sources 268 (2014) 700-705.
[24] Q. An, Q. Wei, L. Mai, J. Fei, X. Xu, Y. Zhao, M. Yan, P. Zhang, S. Huang, Phys. Chem. Chem. Phys. 15 (2013) 16828-16833.
[25] R. Yu, C. Zhang, Q. Meng, Z. Chen, H. Liu, Z. Guo, ACS Appl. Mater. Interfaces 5 (2013) 12394-12399.
[26] A.Q. Pan, H.B. Wu, L. Yu, X.W. Lou, Angew. Chem. Int. Ed. 52 (2013) 2226-2230.
[27] D.W. Liu, Y.Y. Liu, B.B. Garcia, Q.F. Zhang, A.Q. Pan, Y.H. Jeong, G.Z. Cao, J. Mater. Chem. 19 (2009) 8789-8795.
[28] J.S. Chen, Y.L. Tan, C.M. Li, Y.L. Cheah, D.Y. Luan, S. Madhavi, F.Y.C. Boey, L.A. Archer, X.W. Lou, J. Am. Chem. Soc. 132 (2010) 6124-6130.
[29] A.Q. Pan, H.B. Wu, L. Zhang, X.W. Lou, Energy Environ. Sci. 6 (2013) 1476.
[30] B. Alonso, J. Livage, J. Solid State Chem. 148 (1999) 16-19.
[31] W. Wang, B. Jiang, L.W. Hu, Z.S. Lin, J.G. Hou, S.Q. Jiao, J. Power Sources 250 (2014) 181-187.
[32] L. Soltane, F. Sediri, Mater. Res. Bull. 53 (2014) 79-83.
[33] L. Mai, Y. Gu, C. Han, B. Hu, W. Chen, P. Zhang, L. Xu, W. Guo, Y. Dai, Nano Lett. 9 (2009) 826-830.
[34] A. Odani, V.G. Pol, S.V. Pol, M. Koltypin, A. Gedanken, D. Aurbach, Adv. Mater. 18 (2006) 1431-1436.
[35] M.J. Armstrong, D.M. Burke, T. Gabriel, C. O'Regan, C. O'Dwyer, N. Petkov, J.D. Holmes, J. Mater. Chem. A 1 (2013) 12568-12578.
[36] D. Pham-Cong, K. Ahn, S.W. Hong, S.Y. Jeong, J.H. Choi, C. H. Doh, J.S. Jin, E.D. Jeong, C.R. Cho, Curr. Appl. Phys. 14 (2014) 215-221.
[37] C.F. Zhang, Z.X. Chen, Z.P. Guo, X.W. Lou, Energy Environ. Sci. 6 (2013) 974-978.

Prof. Shuquan Liang received his Ph.D. degree from Central South University (PR China) in 2000. He has been the Dean of School of Materials Science and Engineering at Central South University since 2010. He is the winner of Monash University Engineering Sir John Medal. In the last five years, he developed a research group on the Vanadium-based nanomaterials as cathodes for lithium batteries. He hosted 5 state research projects including national 973 and national 863 projects. He has published more than 60 papers in peer-reviewed journals such as Energy & Environmental Science and Journal of Materials Chemistry. Currently, his main research interests include micro/nanostructured functional materials, nanocomposites and energy storage and conversion devices.

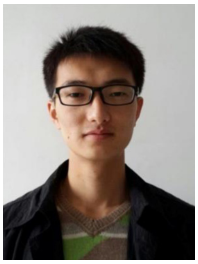

Yang Hu received his B.E. in Materials Science and Engineering from Central south university (PR China) in 2013. Currently, under the guidance of Prof. Liang, he is studying for his Ph.D. Degree in Materials Physics and Chemistry in Central South University. His current research interest is nanostructured cathode materials for lithium ion batteries.

Zhiwei Nie is now a postgraduate student at the School of Materials Science and Engineering, Central South University (PR China). His current research interest is the synthesis of hollow-structured materials for lithium ion batteries.

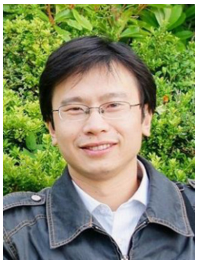

Dr. Han Huang received his BE degree at National University of Defense Technology China in 2002 and Ph.D degree from Physics Department at Zhejiang University, China in 2008. He is currently a professor of physics at Central South University in Changsha China following a six-year research career in National University of Singapore. His current research interests include molecule–substrate interface problems associated with molecular electronics, as well as fabrication and modification of graphene, graphene nanoribbons and other 2-dimensional materials.

Tao Chen received the M.A. from Central South University in 2013, and B.S. from Shanxi University of Science and Technology of China (PR China) in 2010. Currently, he is a Ph.D. candidate under the supervision of Prof. Shuquan Liang at the School of Materials Science and Engineering of Central South University (PR China). His research interests focus on the synthesis of nanostructured materials for lithium ion batteries.

Anqiang Pan received his B. E. (2005) and D. Phil. (2011) degrees in Materials Physics and Chemistry from Central South University in Prof. Shuquan Liang's group. In 2008, he worked in Prof. Guozhong Cao's group at University of Washington as an exchange student (2008–2009). Then, he got the chance to work in PNNL as a visiting scholar in Dr. Ji-Guang Zhang and Dr. Jun Liu's group (2009–2011). After getting the PhD degree, he joined Prof. Xiongwen (David) Lou's group at Nanyang Technological University as a research fellow (2011–2012). He joined the faculty at Central South University in 2012 and was promoted to a Sheng-Hua Professor in 2013. His current interests are the controllable synthesis of nanostructured materials and their applications in energy storage and conversion devices, such as lithium ion batteries, and supercapacitors.

Guozhong Cao is Boeing-Steiner professor of Materials Science and Engineering, professor of Chemical Engineering and adjunct professor of Mechanical Engineering at the University of Washington, Seattle, WA, and also a senior professor at Beijing Institute of Nanoenergy and Nanosystems and a professor at Dalian University of Technology, China. His current research focused on chemical processing of nanomaterials for solar cells, batteries, and supercapacitors as well as actuators and sensors.